PLOS ONE

RESEARCH ARTICLE

Highly efficient photocatalytic degradation of methylene blue by PoPD/TiO_2 nanocomposite

Chuanxi Yang[1,2☯‡], Ming Zhang[3☯‡], Wenping Dong[4], Guanwei Cui[5], Zongming Ren[1,6*], Weiliang Wang[1,6*]

1 College of Geography and Environment, Shandong Normal University, Jinan, People's Republic of China, **2** College of Resources and Environmental Sciences, China Agricultural University, Beijing, People's Republic of China, **3** NJTECH Environment Technology Co., Ltd, Nanjing, People's Republic of China, **4** Shandong Academy of Environmental Science and Environmental Engineering Co., Ltd, Jinan, People's Republic of China, **5** College of Chemistry, Chemical Engineering and Materials Science, Key Laboratory of Molecular and Nano Probes, Ministry of Education, Shandong Normal University, Jinan, People's Republic of China, **6** Institute of Environment and Ecology, Shandong Normal University, Jinan, People's Republic of China

☯ These authors contributed equally to this work.
‡ These authors are co-first authors on this work
* zmren@sdnu.edu.cn (ZMR); sdqcsdnu@163.com (WLW)

Citation: Yang C, Zhang M, Dong W, Cui G, Ren Z, Wang W (2017) Highly efficient photocatalytic degradation of methylene blue by PoPD/TiO_2 nanocomposite. PLoS ONE 12(3): e0174104. https://doi.org/10.1371/journal.pone.0174104

Editor: Yogendra Kumar Mishra, Institute of Materials Science, GERMANY

Received: December 14, 2016

Accepted: March 4, 2017

Published: March 22, 2017

Data Availability Statement: All relevant data are within the paper.

Funding: This work was financially supported by the National Natural Science Foundation of China (41672340). Authors [Zhang Ming] are supported in the form of salary by NJTECH Environment Technology Co., Ltd. Authors [Dong Wenping] are supported in the form of salary by Shandong Academy of Environmental Science and Environmental Engineering Co, Ltd. The specific roles of these authors are articulated in the 'author contributions' section. The funders had no role in

Abstract

The poly-o-phenylenediamine (PoPD)/TiO_2 nanocomposite was successfully synthesized via 'in situ' oxidative polymerization method. The modified photocatalysts were characterized by BET, scanning electron microscopy (SEM), transmission electron microscopy (TEM), X-ray diffraction (XRD), Fourier-transform infrarad spectra (FT-IR), thermogravimrtic analysis (TGA), X-ray photoelectron spectroscopy (XPS), Ultraviolet-visible diffuse reflectance spectrum (UV-Vis DRS) and Photocurrent Test. The results showed that the PoPD exists on the surface of TiO_2, the presence of PoPD does not impact on the lattice structure and grain size of TiO_2, and the presence of PoPD enhances the visible response and photoelectric property. The photocatalytic degradation of methylene blue (MB) was chosen as a model reaction to evaluate the photocatalytic activities of TiO_2 and PoPD/TiO_2. The optimal preparation condition was the molar ratio of oPD to TiO_2 = 3:1, HCl concentration = 1.2 mol/L, the molar ratio of APS to oPD = 1:1. The apparent first-order rate constant k_{app} of PoPD/TiO_2 nanocomposite was 0.0098 min^{-1}, which is 6 times higher than TiO_2 (0.0016 min^{-1}). Meanwhile, the PoPD/TiO_2 nanocomposites showed excellent photocatalytic stability, and the photocatalytic stability was depended on the stability of structure. At last, the photocatalytic mechanism of POPD/TiO_2 nanocomposites was also proposed based on the synergetic effect between TiO_2 and PoPD.

Introduction

Semiconductor as a high-profile photocatalyst has been widely applied in various areas ranging from solar cell to water pollution control [1–3]. Recent research showed that TiO_2-based heterogeneous photocatalytic oxidation technologies are still the most promising methods because of their outstanding oxidative power and stability [4–6]. During recent decades,

study design, data collection and analysis, decision to publish, or preparation of the manuscript.

Competing interests: We declare that we do not have any commercial or associative interest that represents a conflict of interest in connection with the work submitted. The co-first author, Zhang Ming, as employed in NJTECH Environment Technology Co., Ltd, provided support in the form of salary for authors. The third author, Dong Wenping, as employed in Shandong Academy of Environmental Science and Environmental Engineering Co, Ltd, provided support in the form of salary for authors. There are no patents, products in development, or marketed products to declare. This does not alter our adherence to PLOS ONE policies on sharing data and materials.

enormous efforts have been devoted to developing a series of semiconductor photocatalysts, such as TiO_2, ZnO, CdS, and so on [7–10]. However, slow reaction rate, poor solar efficiency, the low quantum efficiency, the critical drawback of photocorrosion, and secondary pollution on the environment impaired their applications to a great extent [11–12]. To eliminate these drawbacks, many attempts have been carried out to modify surface of TiO_2, such as doping, metal deposition, compound semiconductor, and conducting polymer modifying [13].

Recently, the properties of conducting polymer in electron-transfer processes have been widely studied to show they can efficiently arouse a rapid photoinduced charge separation and a relatively slow charge recombination [14]. Zhang Hao et al. and Lin Yangming et al. prepared PANI/TiO_2 nanocomposites and they found the as-prepared samples have enhanced photocatalytic activity under visible light [15–16]. Li Xueyan et al. and Wang Desong et al. prepared PANI/TiO_2 and PPY/TiO_2 nanocomposites via 'in situ' oxidative polymerization method and then indicated composite photocatalyst with excellent photocatalytic performance was attributed to the sensitizing effect of conducting polymer, and the synergetic effect between conducting polymer and TiO_2 [17–18].

In addition to PANI and PPY, poly-o-phenylenediamine (PoPD) was also paid attehtion to the research of conducting polymer modified TiO_2 to improve its photocatalytic performance [19]. As a typical conducting polymer, PoPD has attracted considerable attention since its discovery. Taking advantage of the unique electrical, optical and photoelectric properties of PoPD, we expect that the combination of PoPD with TiO_2 may induce an interesting charge transfer and thus enhance the photocatalytic activity of TiO_2 under visible light irradiation [20]. However, the photocatalytic activity enhanced mechanism has not been studied. The photocatalytic process of PoPD/TiO_2 involves a primary reaction process that generates holes and electrons and a secondary reaction process that generates reactive oxygen species [21]. Therefore, achieving a quantitative estimate of the contributions of PoPD under the primary and secondary reaction processes is important [22].

However, in most cases, the photocatalytic degradation of organic pollutants was mainly for organic dyestuff, and little research was performed on phenols, highly toxic and carcinogenic compounds, meanwhile the mechanism of PoPD/TiO_2 nanocomposite photocatalyst under the visible light has not been convincingly explained [23].

In this study, PoPD/TiO_2 nanocomposite was successfully synthesized via 'in situ' oxidative polymerization method. The modified photocatalysts were characterized by BET, scanning electron microscopy (SEM), transmission electron microscopy (TEM), X-ray diffraction (XRD), Fourier-transform infrarad spectra (FT-IR), thermogravimrtic analysis (TGA), X-ray photoelectron spectroscopy (XPS), Ultraviolet-visible diffuse reflectance spectrum (UV-Vis DRS) and Photocurrent Test. The photocatalytic degradation of methylene blue (MB) was chosen as a model reaction to evaluate the photocatalytic activities of TiO_2 and PoPD/TiO_2, results indicated that the PoPD/TiO_2 nanocomposites showed excellent photocatalytic activity and stability. Meanwhile, the photocatalytic mechanism of POPD/TiO_2 nanocomposites was also proposed based on the synergetic effect between TiO_2 and PoPD. It hoped our works could provide valuable information on the synthesis and application of conducting polymer modified semiconductor.

Materials and methods

Materials

The o-phenylenediamine (oPD), ammonium persulfate (APS), sulfuric acid (H_2SO_4) and sodium hydroxide (NaOH) were purchased from Tianjin Kermel Chemical Reagent Co., Ltd. The anatase TiO_2 was purchased from Aladdin Chemical Reagent Co., Ltd. The ethyl alcohol

was purchased from Tianjin Fuyu Fine Chemical Co., Ltd. The hydrochloric acid was purchased from Sinopharm Chemical Reagent Co., Ltd. The methylene blue (MB) was purchased from Tianjin Guangcheng Chemical Reagent Co., Ltd. All chemicals are analytical grade without further purification. Deionized water was used for the synthesis of all solutions.

Sample synthesis

The typical synthesis of PoPD/TiO_2 nanocomposite photocatalyst was as follows: An appropriate amount of oPD was dissolved in 90 ml 1.2 mol/L hydrochloric acid solution, with 0.256 g anatase TiO_2 adding. The solution was ultrasonic cleaning 15 min to mixing uniformity. After dissolving, the solution was labeled A. An appropriate amount of APS was dissolved in 30 ml 1.2 mol/L hydrochloric acid solution, the solution was labeled B. The solution A was transferred to a 250 ml round-bottom flask, magneton was added, and the solution was stirred with a magnetic stirrer. The solution B was transferred to a 100 ml constant pressure funnel and then dropped in solution A at about 1drop/second with stirring. The reaction was continued with 24 h at room temperature. The final products were filtered and washed with deionized water and ethanol and dried at 80˚C for several hours in a vacuum oven.

Characterization

The surface texture of TiO_2 and PoPD/TiO_2 nanocomposite was examined by N_2 adsorption at 77 K (Quantachrome instruments Quadrasorb SI). The specific surface area was calculated from the N_2 adsorption isotherm using the BET equation. Scanning electron microscope (SEM) patterns were performed on a QUANTA F250 cold field emission scanning electron microscope. Transmission electron microscopy (TEM) patterns were performed on a FEI Tecnai G2 20 transmission electron microscopy. X-Ray Diffraction (XRD) patterns were recorded on a Bruker D8 Advance X-ray diffractometer with Cu Kα radiation. Fourier-transform infrarad spectra (FT-IR) of the samples were recorded on Vertex 70 spectrometer in a range from 4000 to 400 cm^{-1}. Thermogravimetric analysis (TGA) of all of the samples were performed with a Q500 thermal analysis instrument (TA instruments Co., Ltd.). The samples were heated from 35 to 800˚C at a rate of 10˚C min^{-1} in air. X-ray photoelectron spectroscopy (XPS) measurements were performed using a Thermo ESCALAB 250Xi system with an Al Kα X-ray source. All of the binding energies were referenced to the C1s peak at 284.8 eV for the surface adventitious carbon. Ultraviolet-visible diffuse reflectance spectrum (UV-Vis DRS) were detected by an UV-2550PC ultraviolet and visible spectrophotometerwith $BaSO_4$ as the background ranging from 200 to 800 nm. Photocurrent test was measured using a CHI660D VersaSTAT. The TiO_2 and PoPD/TiO_2 nanocomposites were deposited as a film on a 2 cm × 2 cm indium-tin-oxide conducting glass to obtain the working electrode. The saturated calomel electrode and Pt electrode served as the reference electrode and the counter electrode, respectively. The electrolyte was 0.1 mol/L Na_2SO_4 solution.

Photocatalytic activity test

The photocatalytic activity was evaluated by the decomposition of MB under visible light (λ >450 nm). The visible light was obtained by a 1000W xenon lamp (XPA-II Photochemical Reactions Instrument) with a 400 nm cutoff filter to ensure the desired irradiation light. Aqueous suspensions of MB (30 mL, 10 mg/L) were placed in a quartz tube, and 30 mg of PoPD/TiO_2 nanocomposite photocatalyst were added. Prior to irradiation, the suspensions were magnetically stirred in darkness for about 3 h. The suspensions were kept under constant air-equilibrated conditions before and during illumination. At certain time intervals, 1 mL liquor was sampled and centrifuged to remove the particles. The filtrates were analyzed by recording

variations of the maximum absorption band (664 nm for MB) using a UV-2550PC ultraviolet and visible spectrophotometer. To evaluate the accuracy the PoPD/TiO_2 nanocomposite photocatalyst, the photocatalytic process was reused four times to degrade MB under visible light.

Results

Physicochemical properties of PoPD/TiO_2 nanocomposite

It was well-known that the photocatalytic activity was governed by various factors such as surface area, phase structure, interfacial charge transfer, and separation efficiency of photoinduced electrons and holes. The adsorption and desorption isotherms of N_2 at 77 K on TiO_2 and PoPD/TiO_2 nanocomposites, are shown in Fig 1. Like the anatase TiO_2, the PoPD/TiO_2 nanocomposite also displays a Type II isotherm characteristic of a mesoporous material [24]. Clearly the total pore volume and surface area of PoPD/TiO_2 nanocomposite are much less than those of TiO_2. However, the PoPD/TiO_2 nanocomposite showed the higher photocatalytic activity than TiO_2, indicating that the surface area of photocatalyst is only an index to character the physicochemical properties, not the decisive index to ensure the photocatalytic activity.

Fig 2 shows the SEM images of TiO_2 and PoPD/TiO_2 nanocomposites. Compared with TiO_2 (Fig 2A and 2B), PoPD/TiO_2 nanocomposite (Fig 2C and 2D) possessed of more smooth interface, indicating that TiO_2 and PoPD layer formed the core-shell structure. The grain size was about 30–50 nm, and SEM patterns of TiO_2 and PoPD/TiO_2 showed no change before and after modification by PoPD, indicating that the deposited PoPD layer was very thin. There were agglomeration phenomena discernable because the grain size was small and the stong acting force (Van der Waals' Force and electrostatic attraction). Compared with TiO_2, PoPD/TiO_2 composite photocatalyst possessed a low dispersion degree and obvious agglomeration phenomenon because of the oxidation polymerization reaction and PoPD conglutination.

Fig 3 shows the TEM images of TiO_2 and PoPD/TiO_2 nanocomposites. From the results shown in Fig 3A, 3B, 3C and 3D, there were agglomeration phenomena of PoPD/TiO_2

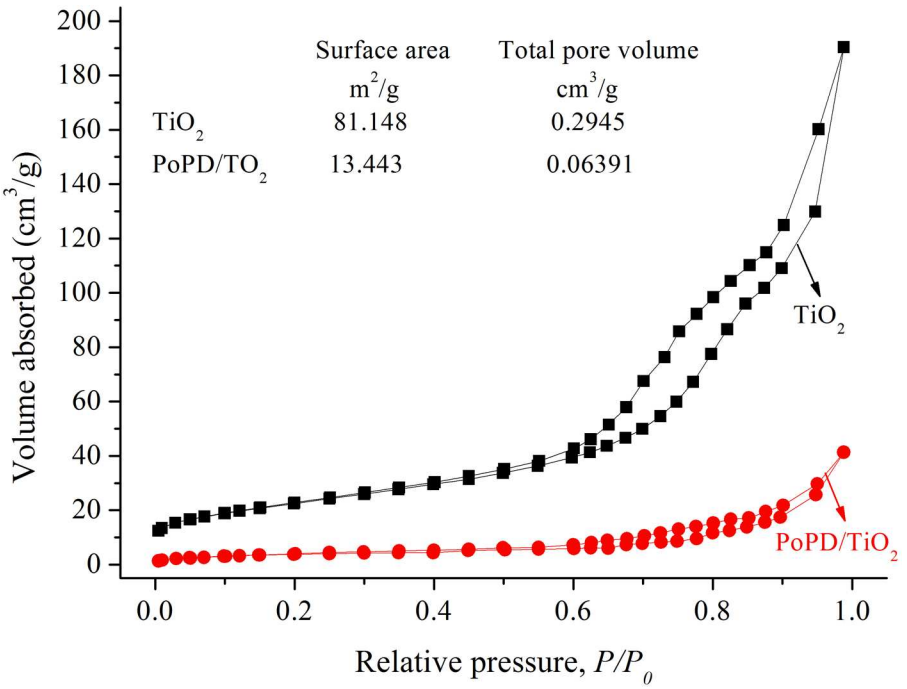

Fig 1. N_2 adsorption and desorption isotherms at 77 K onTiO_2 and PoPD/TiO_2.

https://doi.org/10.1371/journal.pone.0174104.g001

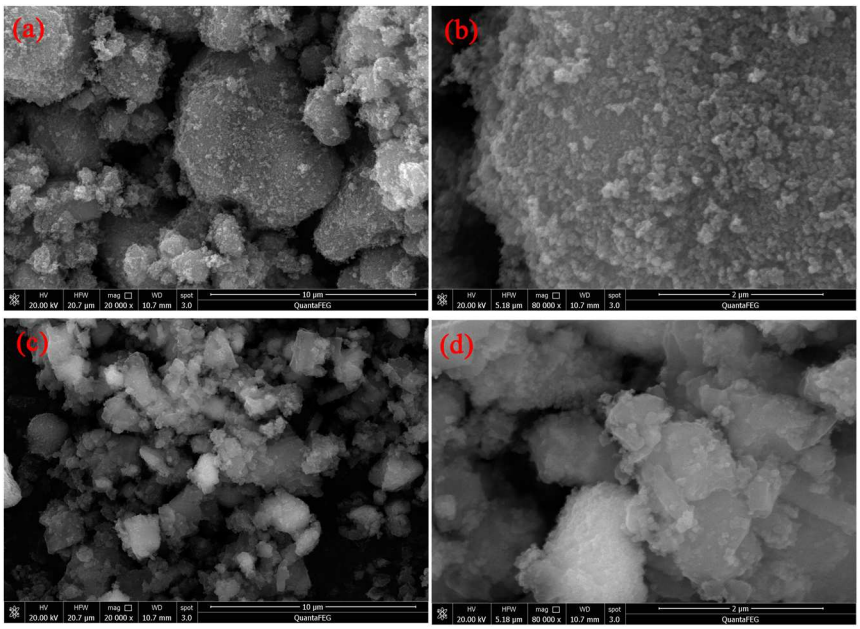

Fig 2. SEM images of (a-b) TiO_2 and (c-d) PoPD/TiO_2 nanocomposites.

https://doi.org/10.1371/journal.pone.0174104.g002

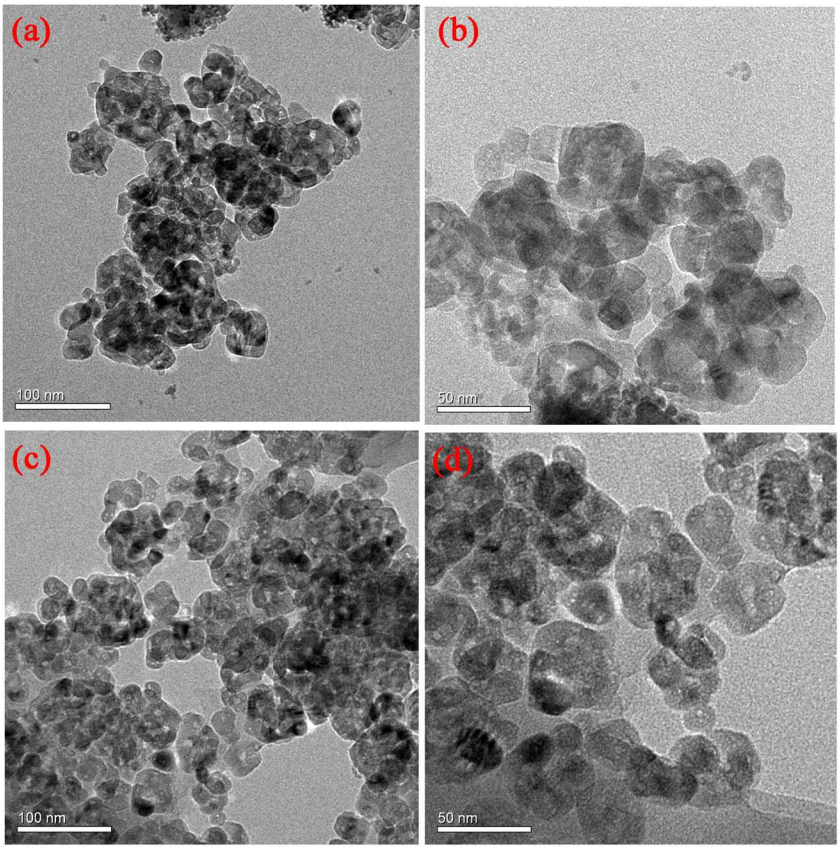

Fig 3. TEM images of (a-b) TiO_2 and (c-d) PoPD/TiO_2 nanocomposites.

https://doi.org/10.1371/journal.pone.0174104.g003

nanocomposite observable because of high surface energy. The grain size of PoPD/TiO_2 nanocomposite observed in TEM images was about 30–50 nm, and the result was consistent with SEM images.

Fig 4 shows the XRD spectra of TiO_2 and PoPD/TiO_2 nanocomposites. The peaks at 2θ values of 25.3˚, 37.8˚, 48.0˚, 53.9˚, 55.1˚, 62.7˚ 68.8˚, 70.3˚, and 75.0˚ can be indexed to (101), (004), (200), (105), (211), (204), (116), (220), and (215) faces of anatase TiO_2, respectively. It is obvious that the PoPD/TiO_2 nanocomposite has not change in peak positions and shapes compared with the pure TiO_2, indicating that the presence of PoPD does not impact on the lattice structure of TiO_2.

The grain size can be calculated by the following Scherrer Equation:

$$D = \frac{K\lambda}{(\cos\theta \bullet B_{1/2})} \quad (1)$$

where D represents grain size, K is the Scherrer constant of diffraction peak and the value of anatase TiO_2 crystal is 0.89, λ represents the wavelength of X ray, $B_{1/2}$ is full width at half maximum of diffraction peak, θ is the Bragg Diffraction Angle. Based on the (101) face main peak at 2θ value of 25.3˚ of PoPD/TiO_2 photocatalyst, the calculated grain size was 44.6 nm. Comparing with calculated the grain size of anatase TiO_2 crystal (44.2 nm), the presence of PoPD does not impact on the grain size of TiO_2.

The FT-IR spectra of TiO_2, PoPD, and PoPD/TiO_2 are shown in Fig 5. The main characteristic bands of PoPD are assigned as follows: the peak at 1629 cm^{-1} is associated with C = N stretching vibration, and the strong absorption band at 1523 cm^{-1} is ascribed to the C = C stretching vibrations in the benzene ring. The weak peaks at 1328 cm^{-1} and 1238 cm^{-1} are correspondingly assigned to the = C-N stretching on the benzene ring. The FT-IR spectrum of the PoPD/TiO_2 contains the same main characteristic bands as that of PoPD but with a shift to higher wavenumbers [25]. The results show that there is a strong interaction between PoPD

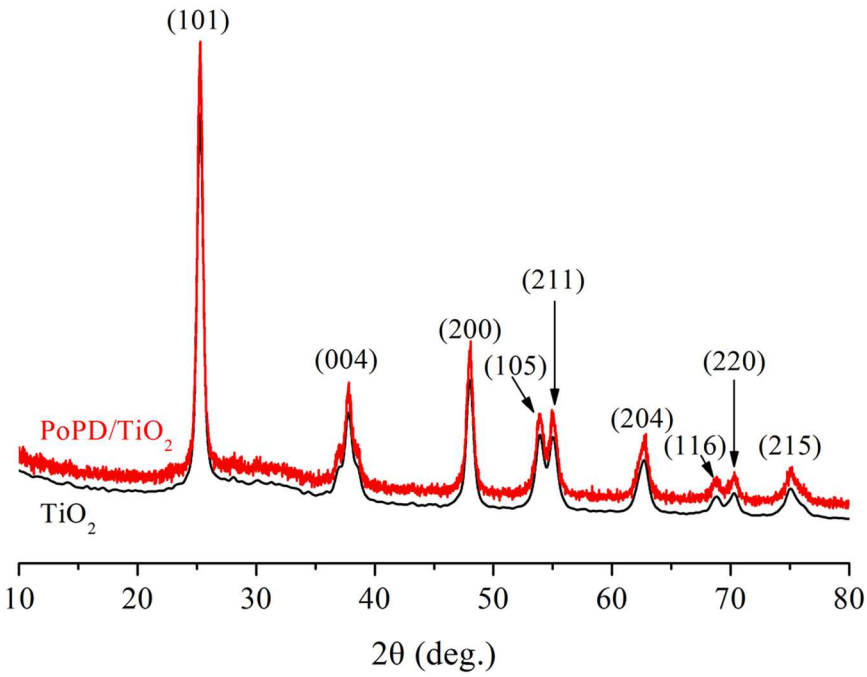

Fig 4. XRD pattern of TiO_2 and PoPD/TiO_2 nanocomposites.

https://doi.org/10.1371/journal.pone.0174104.g004

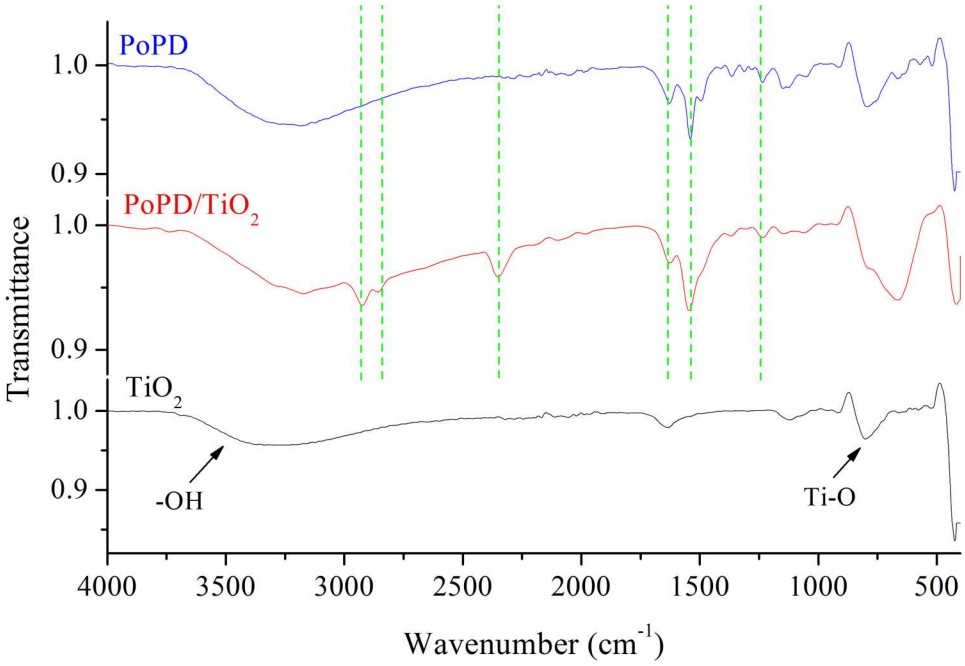

Fig 5. FT-IR spectra of TiO_2, PoPD, and PoPD/TiO_2 nanocomposites.

https://doi.org/10.1371/journal.pone.0174104.g005

and the TiO_2 nanoparticles (2350 cm^{-1}, 2850 cm^{-1}, and 2925 cm^{-1}), and the PoPD deposits and forms a shell on the surface of the TiO_2 nanoparticles. The deposition of PoPD on the surface of the TiO_2 nanoparticles not only constrains the motion of the PoPD chains but also restricts the vibration mode in the PoPD molecule. It can be observed that the characteristic band of TiO_2 at 745 cm^{-1} (Ti-O) occurred in the PoPD/TiO_2 nanocomposite and the band is so wide that it hides the figure peak in the PoPD/TiO_2 nanocomposite.

The thermal behavior of TiO_2 and PoPD/TiO_2 was investigated by TGA, and the results are shown in Fig 6. In Fig 6, curve (a) indicates that TiO_2 is very stable in air, and no decomposition occurred in the 30–800˚C range. The thermogravimetric curve of PoPD/TiO_2 is shown in Fig 6(B). The first weight loss was observed at 100˚C owing to desorption of the water that was absorbed on PoPD/TiO_2 nanocomposite This curve also indicates that a sharp weight loss occurs at approximately 450˚C and continues up to 600˚C. This weight loss was due to decomposition of PoPD.

X-ray photoelectron spectroscopy (XPS) is an important tool for studying the electronic structure of condensed matter and is widely used for quantitative surface analysis. According to the XPS survey spectra (Fig 7) of TiO_2 and PoPD/TiO_2, Ti and O were present in TiO_2 based on the two peaks at binding energies of 458.5 and 529.8 eV. In addition, the C, O, Ti and N elements existed in the TiO_2 based on the four peaks with binding energies of 284.8, 529.8, 458.5 and 400.3 eV, which are related to C1s, O1s, Ti2p and N1s, respectively [26]. The atomic percentages of C, O, Ti and N were 52.55%, 22.98%, 10.92% and 13.55%, respectively, suggesting that PoPD exists on the TiO_2 surface.

To obtain information about response to ultraviolet light and visible light of the samples, TiO_2 and PoPD/TiO_2 nanocomposites were characterized by UV-Vis DRS. As shown in Fig 8, it can be observed that both TiO_2 and PoPD/TiO_2 had strong responses to UV light, but PoPD/TiO_2 had the stronger responses to visible light. Meanwhile, there was an absorption peak at 460 nm of PoPD/TiO_2. The results not only proved the existence of PoPD on the TiO_2

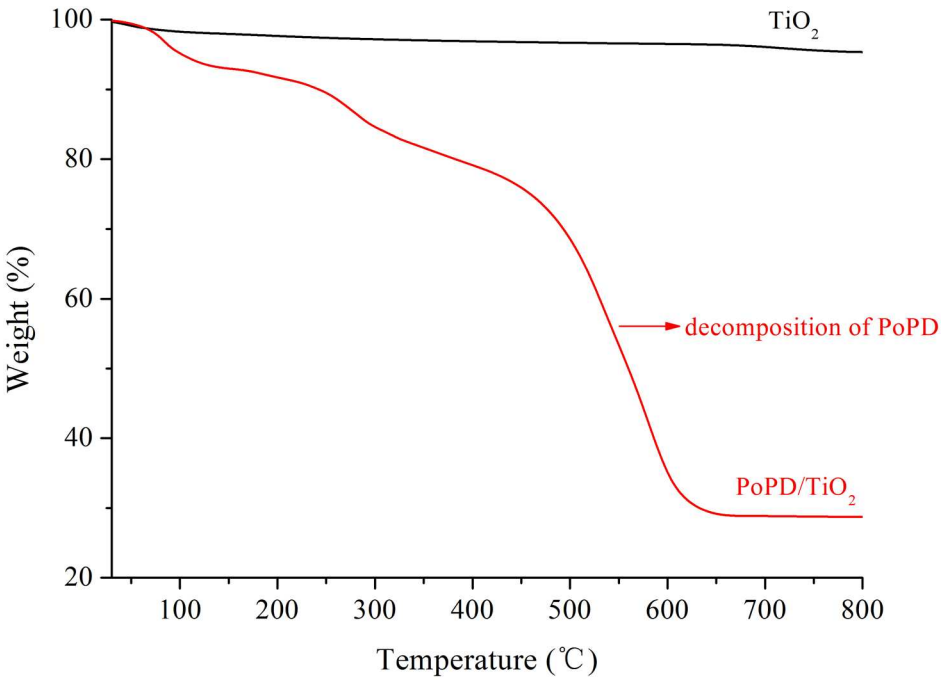

Fig 6. TGA curves of (a) TiO_2 and (b) PoPD/TiO_2 nanocomposites.

https://doi.org/10.1371/journal.pone.0174104.g006

surface, but also explained the reason why PoPD/TiO_2 had the higher photocatalytic performance than TiO_2 under visible light [27].

To obtain information of photoelectric property, TiO_2 and PoPD/TiO_2 nanocomposites were characterized by Photocurrent Test. As shown in Fig 9, the photocurrent density of TiO_2

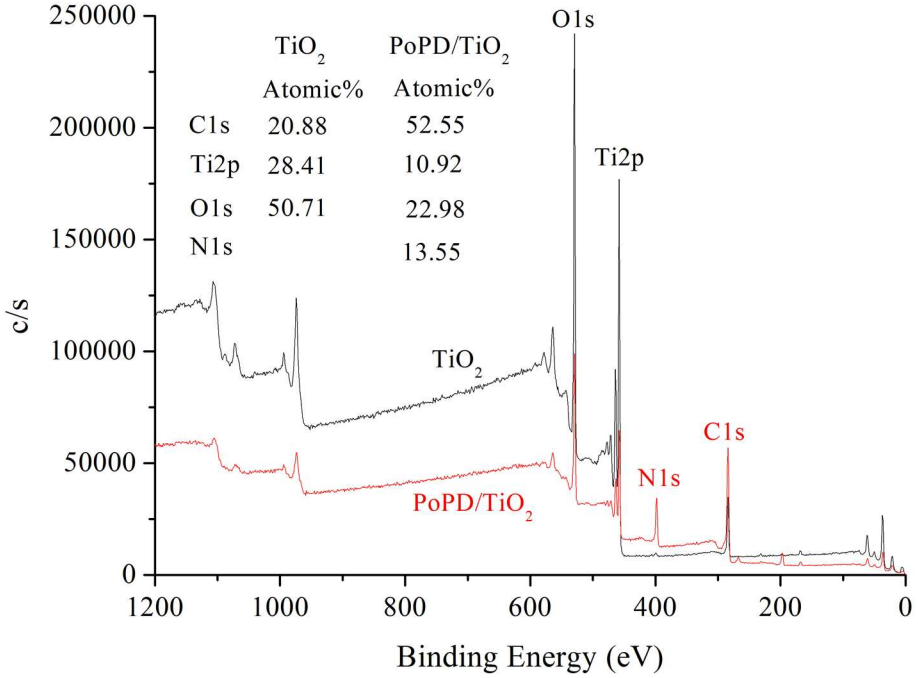

Fig 7. XPS spectra of TiO_2 and PoPD/TiO_2 nanocomposites.

https://doi.org/10.1371/journal.pone.0174104.g007

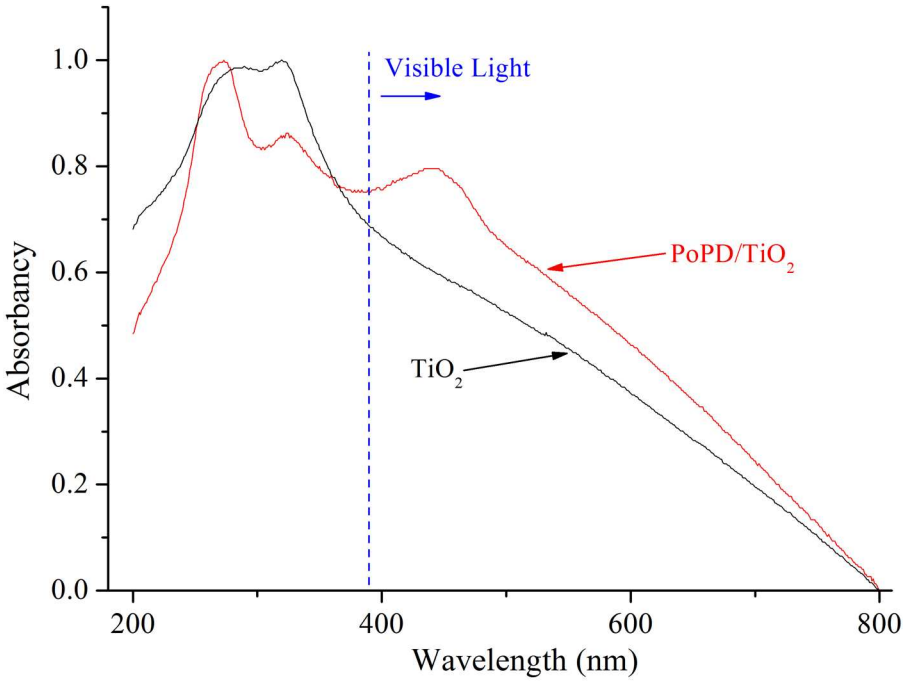

Fig 8. UV-Vis DRS of TiO_2 and PoPD/TiO_2 nanocomposites.

https://doi.org/10.1371/journal.pone.0174104.g008

was low (about 1μA/cm^2) under visible light because the pure TiO_2 band gap was about 3.2 eV, but photocurrent density of PoPD/TiO_2 nanocomposite under visible light was 7 times as high as pure TiO_2. The results indicated that there was a heterostructure between TiO_2 and PoPD

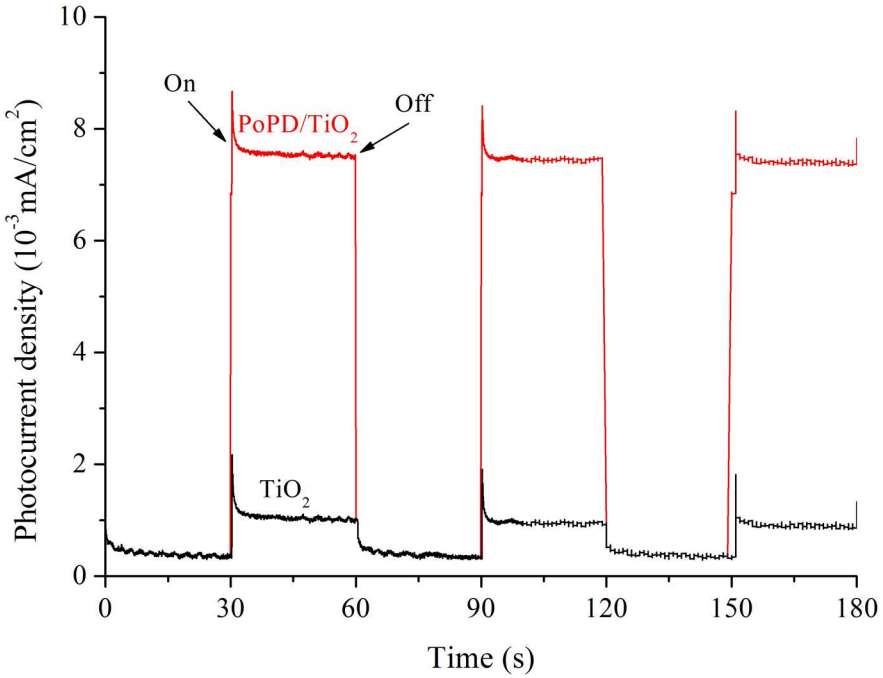

Fig 9. Photocurrent density of TiO_2 and PoPD/TiO_2 nanocomposites under visible light irradiation.

https://doi.org/10.1371/journal.pone.0174104.g009

to possessing the strong responses to visible light and producing abundant hole-electron pairs. The PoPD had excellent electrical conductivity to transfer free electrons from VB to CB, showing the PoPD/TiO_2 had higher photocurrent density and photocatalytic performance than TiO_2. Similar results were also obtained with the research of Liao et al about photonic crystal coupled TiO_2/polymer hybrid for efficient photocatalysis under visible light irradiation [28–29]. The results proved that the combination of TiO_2 and PoPD was an effective way to improve photocatalytic activity.

Photocatalytic activity of PoPD/TiO_2 nanocomposite

The photocatalytic performance of PoPD/TiO_2 nanocomposites for liquid-phase degradation of MB has been measured for the molar ratio of oPD to TiO_2, the concentration of hydrochloric acid, and the molar ratio of APS to oPD. MB has a maximum absorption at about 664 nm.

The influences of molar ratios of oPD to TiO_2 in the oxidative polymerization reaction to PoPD/TiO_2 photocatalytic performance are shown in Fig 10(A). The influences of the concentration of hydrochloric acid in the oxidative polymerization reaction to PoPD/TiO_2 photocatalytic performance are shown in Fig 10(B). The influences of the molar ratios of APS to oPD in the oxidative polymerization reaction are shown in Fig 10(C). The kinetics plots are shown by apparent first-order linear transform $-\ln(C/C_0) = k_{app}t$. The activity of TiO_2 and PoPD/TiO_2 nanocomposites can be evaluated by comparing the apparent first-order rate constants (k_{app}) list in Table 1.

As can be seen from the Fig 10 and Table 1, the photocatalytic degrading efficiency was increased with the molar ratio of oPD to TiO_2 increased, but it was decreased when the molar ratio of oPD to TiO_2 was over 3:1. The photocatalytic degrading efficiency was increased with the concentration of hydrochloric acid from 0.6 mol/L to 1.2 mol/L, the photocatalytic degrading efficiency was resembled with the concentration of hydrochloric acid from 1.2 mol/L to 1.8 mol/L, and the photocatalytic degrading efficiency was decreased with the concentration of hydrochloric acid from 1.8 mol/L to 2.4 mol/L. When the molar ratio of APS to oPD was over 1:1, the photocatalytic performance of PoPD/TiO_2 composite photocatalyst decreased with the molar ratio of APS to oPD increased. So the optimal preparation condition was the molar ratio of oPD to TiO_2 3:1, the concentration of hydrochloric acid 1.2 mol/L, and the molar ratio of APS to oPD 1:1.

Photocatalytic stability of PoPD/TiO_2 nanocomposite

To obtain information about the stability of the PoPD/TiO_2 nanocomposite, the recycling experiments were finished. From the results shown in Fig 11, after four times run of

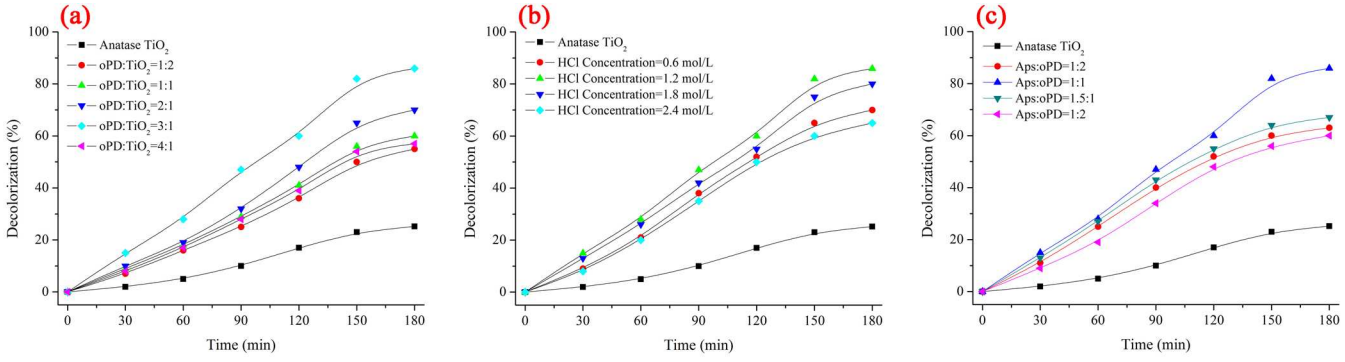

Fig 10. Results of degrading MB using different (a) molar ratios of oPD to TiO_2 nanocomposites, (b) the concentration of hydrochloric acid, and (c) the molar ratio of APS to oPD.

https://doi.org/10.1371/journal.pone.0174104.g010

Table 1. Apparent first-order rate constants (k_{app}) of MB degradation and linear regression coefficients from -ln(C/C_0) = $k_{app}t$.

Samples		-ln(C/C_0) = $k_{app}t$	k_{app}	R^2	$\frac{k_{P/T}}{k_T}$ b
	TiO_2	-ln(C/C_0) = 0.0016t	0.0016	0.9443	
oPD:TiO_2	1:2	-ln(C/C_0) = 0.0041t	0.0041	0.9538	2.56
	1:1	-ln(C/C_0) = 0.0048t	0.0048	0.9556	3.00
	2:1	-ln(C/C_0) = 0.0061t	0.0061	0.9303	3.81
	3:1[a]	-ln(C/C_0) = 0.0098t	0.0098	0.9108	6.13
	4:1	-ln(C/C_0) = 0.0045t	0.0045	0.9559	2.81
HCl	0.6 mol/L	-ln(C/C_0) = 0.0064t	0.0064	0.9600	4.00
	1.2 mol/L[a]	-ln(C/C_0) = 0.0098t	0.0098	0.9108	6.13
	1.8 mol/L	-ln(C/C_0) = 0.0081t	0.0081	0.9297	5.06
	2.4 mol/L	-ln(C/C_0) = 0.0057t	0.0057	0.9676	3.56
Aps:oPD	1:2	-ln(C/C_0) = 0.0058t	0.0058	0.9858	3.63
	1:1[a]	-ln(C/C_0) = 0.0098t	0.0098	0.9108	6.13
	1.5:1	-ln(C/C_0) = 0.0064t	0.0064	0.9872	4.00
	2:1	-ln(C/C_0) = 0.0051t	0.0061	0.9754	3.81

a: The optimal preparation condition is oPD:TiO_2 = 3:1, HCl concentration = 1.2 mol/L, and Aps:oPD = 1:1.

b: The specific value between k_{app} of PoPD/TiO_2 ($k_{P/T}$) and k_{app} of TiO_2 (k_T).

https://doi.org/10.1371/journal.pone.0174104.t001

degradation reaction, the photocatalytic decolourization ratio of MB was decreased from 85.9% to 81.1% after 4 h irradiation under visible light. So the prepared PoPD/TiO_2 nanocomposite possessed excellent photocatalytic stability.

Discussion

Preparation condition and photocatalytic activity of PoPD/TiO_2 nanocomposite

Considered the pure anatase TiO_2 had no response to visible light, the PoPD had response to visible light and excited electrons from valence band (VB) to conduction band (CB), the ·OH free radical were produced in PoPD/TiO_2 to destain and degrade MB.

When the molar ratio of oPD to TiO_2 was low, with the molar ratio of oPD to TiO_2 increasing, the thickness of deposited PoPD on TiO_2 surface was increasing, so the producing electron-hole pairs accumulated, and the photocatalytic performance was stronger. However, when the molar ratio of oPD to TiO_2 continued to increase, the thickness of deposited PoPD on the TiO_2 surface was too thick to influence the transmission of producing electron, so the photocatalytic performance of PoPD/TiO_2 nanocomposite decreased.

It was well-known that hydrochloric acid not only provides the acidity in oxidative polymerization reaction, but also the electrolytic Cl^- can mix into intramembrane to neutralize the positive charge [30]. The Cl^- mixing can avail the charge delocalization in the PoPD molecular chain to enhance the electrical conductivity of PoPD. However, when the concentration of hydrochloric acid was too high, the mixing amount was troppo to influence the contact between oPD molecules. Then the results led to the molecular chain shortening and electrical conductivity decreasing, which led to the photocatalytic performance of PoPD/TiO_2 decreased.

When the molar ratio of APS to oPD was low in the PoPD oxidative polymerization reaction, considered lack of the active sites for the reaction, the oxidative polymerization reaction was inclined to produce macromolecule PoPD, so the conductivity and productivity of PoPD increased with the amount of APS increased. When the molar ratio of APS to oPD was too

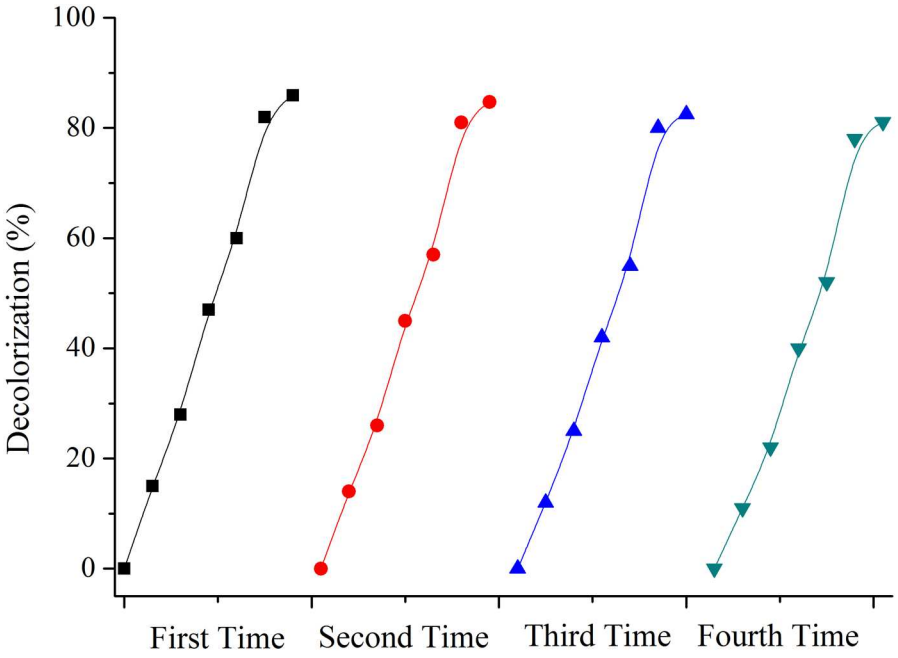

Fig 11. Photocatalytic degradation rate of MB with PoPD/TiO_2 nanocomposites in different recycling time.

https://doi.org/10.1371/journal.pone.0174104.g011

high in the PoPD oxidative polymerization reaction, not only the superfluous active sites for the reaction were led to the disadvantage of producing macromolecule PoPD, but also the superfluous APS oxidated the main molecular chain to break the conjugated structure. So the reaction was led to a decrease in the conductivity and productivity of PoPD, and the photocatalytic performance of PoPD/TiO_2 decreased [31].

Photocatalytic stability of PoPD/TiO_2 nanocomposite

In order to ensure the photocatalytic stability of PoPD/TiO2 nanocomposite, the FT-IR spectra and XRD patterns before and after reaction were redorded as shown in Fig 12. It is found that the shape of FT-IR and XRD after photocatalytic reaction is similiar to that before reaction. It indicates that the structure of PoPD/TiO_2 nanocomposite does not change during the photocatalytic process, and the stability of photocatalytic activity is depended on the stability of structure.

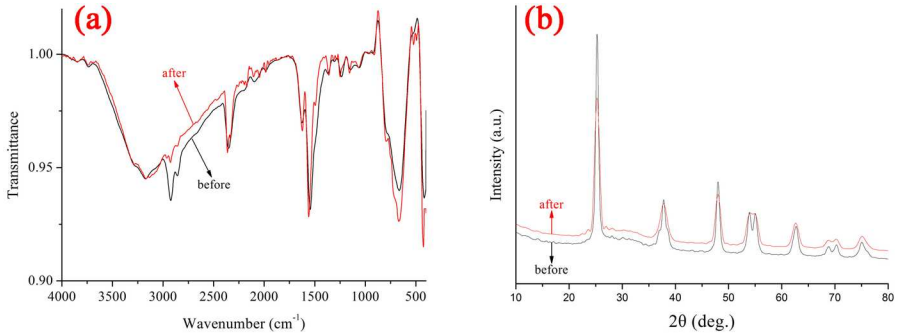

Fig 12. (a) FT-IR spectra and (b) XRD patterns of PoPD/TiO_2 nanocomposites before and after photocatalytic reaction.

https://doi.org/10.1371/journal.pone.0174104.g012

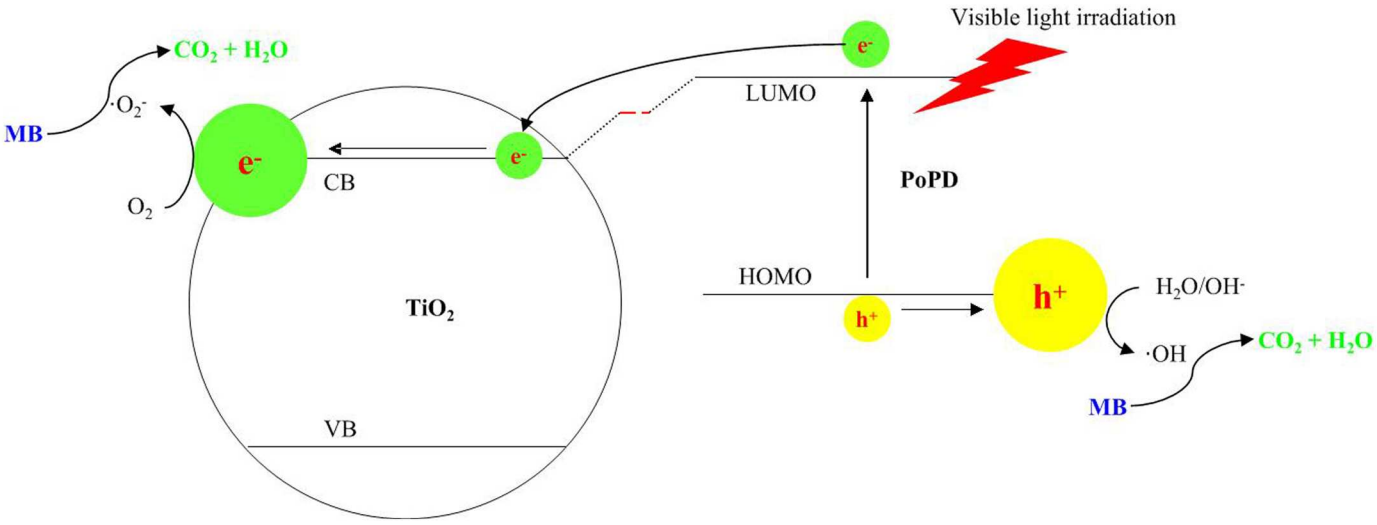

Fig 13. Photocatalytic mechanism of PoPD/TiO_2 nanocomposites to enhance photocatalytic activity under visible light irradiation.

https://doi.org/10.1371/journal.pone.0174104.g013

Photocatalytic mechanism

The synergetic effect between TiO_2 and PoPD on the photocatalytic degradation of MB exists clearly for all the PoPD/TiO_2 nanocomposites. The mechansim of PoPD on the activity of the PoPD/TiO_2 nanocomposites can be explained as photosensitizer (Fig 13). It was well-known that TiO_2 had the special energy-band structure which means including valence band (VB) to conduction band (CB). The band-gap energy of anatase TiO_2 was 3.2 eV, indicating that it only had response to small amount light (λ>387 nm). Because PoPD has charge-transfer excitation-like transition from the Highest Occupied Molecular Orbital (HOMO) to the Lowest Unoccupied Molecular Orbital (LUMO) can lead to that itself excited photogenerated electrons transfer to the CB of TiO_2 and it accepts the holes from the VB of TiO_2. On the one hand the photogenerated electrons were transferred to CB to produce e^-_{CB}, on the other hand there were holes (h^+) in VB after electrons transferred to PoPD. The free electrons e^-_{CB} reacted with O_2 to produce superoxide radical $\cdot O_2^-$, and holes h^+ reacted with OH^- and H_2O to produce hydroxyl radical ·OH. And the reactive oxygen species are responsible for the degradation of MB [32–34].

The photocatalytic mechanism of PoPD/TiO_2 nanocomposites under visible light was expounded as following [35–36].

$$PoPD/TiO_2 \xrightarrow{vis-light} PoPD^+/TiO_2 + e^- \quad (2)$$

$$e^- + O_2 \rightarrow \bullet O_2^- \quad (3)$$

$$PoPD^+/TiO_2 \rightarrow PoPD/TiO_2 + h^+ \quad (4)$$

$$h^+ + OH^- \rightarrow \bullet OH \quad (5)$$

$$h^+ + H_2O \rightarrow \bullet OH + H^+ \quad (6)$$

Conclusions

The PoPD/TiO_2 nanocomposites were prepared via 'in situ' oxidative polymerization method using APS as oxidant, oPD as monomers, and anatase TiO_2 particles as titanium source. The optimal preparation conditions included that the molar ratio of oPD to TiO_2 was 3:1, hydrochloric acid concentration was 1.2 mol/L, the molar ratio of APS to oPD was 1:1.

The photocatalysts were characterized by BET, XRD, SEM, TEM, UV-VIS DRS and Photocurrent Test, and the results showed that the PoPD exists on the surface of TiO_2, the presence of PoPD do not impact on the lattice structure and grain size of TiO_2, and the presence of PoPD enhances the visible response and photoelectric property.

The photocatalytic degradation of methylene blue (MB) was chosen as a model reaction to evaluate the photocatalytic activities of TiO_2 and PoPD/TiO_2. The decolorization ratio of MB using PoPD/TiO_2 nanocomposite prepared with optimal preparation condition was 85.9% (apparent first-order rate constant k_{app} was 0.0098 min^{-1}), which is higher than using TiO_2 Photocatalyst (decolorization ratio of MB was 25.2%; apparent first-order tare constant k_{app} was 0.0016 min^{-1}). Meanwhile, the PoPD/TiO_2 nanocomposites showed excellent photocatalytic stability, and the photocatalytic stability was depended on the stability of structure via the FT-IR spectra and XRD patterns before and after photocatalytic reaction. At last, the photocatalytic mechanism of POPD/TiO_2 nanocomposites was also proposed based on the synergetic effect between TiO_2 and PoPD.

Acknowledgments

This work was financially supported by the National Natural Science Foundation of China (41672340).

Author Contributions

Conceptualization: CXY WLW.

Data curation: CXY MZ WLW.

Formal analysis: CXY MZ WLW.

Funding acquisition: WLW.

Investigation: CXY MZ WPD GWC ZMR WLW.

Methodology: CXY MZ WLW.

Project administration: WLW.

Resources: WLW.

Software: CXY MZ WLW.

Supervision: ZMR WLW.

Validation: ZMR WLW.

Visualization: CXY MZ ZMR WLW.

Writing – original draft: CXY MZ ZMR WLW.

Writing – review & editing: CXY MZ WPD GWC ZMR WLW.

References

1. Chen XB, Clemens B (2008) The electronic origin of the visible-light absorption properties of C-, N- and S-doped TiO_2 nanomaterials. Journal of the American Chemical Society 130: 5018–5019. https://doi.org/10.1021/ja711023z PMID: 18361492
2. Fujishima A, Honda K (1972) Electrochemical photolysis of water at a semiconductor electrode. Nature 238: 37–38. PMID: 12635268
3. Reimer T, Paulowicz I, Roder R, Kaps S, Lupan O, Chemnitz S, Benecke W, Ronning C, Adelung R, Mishra YK (2014) Single step integration of ZnO nano-and microneedles in Si trenches by novel flame transport approach: whispering gallery modes and photocatalytic properties. ACS Applied Materials & Interfaces 10: 7806–7815.
4. Tan F, Sun D, Gao J, Zhao Q, Wang XC, Teng F, et al. (2013) Preparation of molecularly imprinted polymer nanoparticles for selective removal of fluoroquinolone antibiotics in aqueous solution. Journal of Hazardous Materials 244: 750–757. https://doi.org/10.1016/j.jhazmat.2012.11.003 PMID: 23177246
5. Mishra YK, Modi G, Cretu V, Postica V, Lupan O, Reimer T, Paulowicz I, Hrkac V, Benecke W, Kienle L, Adelung R (2015) Direct growth of freestanding ZnO tetrapod networks for multifunctional applications in photocatalysis, UV photodetection, and gas sensing. ACS Applied Materials & Interfaces 26: 14303–14316.
6. Pawar RC, Lee CS (2014) Single-step sensitization of reduced graphene oxide sheets and CdS nanoparticles on ZnO nanorods as visible-light photocatalysts. Applied Catalysis B: Environmental 144: 57–65.
7. Zhang S, Chen QY, Jing DW, Wang Y, Guo L (2012) Visible photoactivity and antiphotocorrosion performance of PdS-CdS photocatalysts modified by polyaniline. International Journal of Hydrogen Energy 37: 791–796.
8. Pawar RC, Pyo Y, Ahn SH, Lee CS (2015) Photoelectrochemical properties and photodegradation of organic pollutants using hematite hybrids modified by gold nanoparticles and graphitic carbon nitride. Applied Catalysis B: Environmental 176: 654–666.
9. Chen Q, He QQ, Lv MM, Liu X, Wang J, Lv J (2014) The vital role of PANI for the enhanced photocatalytic activity of magnetically recyclable N-$K_2Ti_4O_9$/$MnFe_2O_4$/PANI composites. Applied Surface Science 311: 230–238.
10. Pawar RC, Khareb V, Lee CS (2014) Hybrid photocatalysts using graphitic carbon nitride/cadmium sulfide/reduced graphene oxide (g-C_3N_4/CdS/RGO) for superior photodegradation of organic pollutants under UV and visible light. Dalton Transactions 33: 12514–12527.
11. Mishra YK, Chakravadhanula VSK, Hrkac V, Jebril S, Agarwal DC, Mohapatra S, Avasthi DK, Kienle L, Adelung R (2012) Crystal growth behaviour in Au-ZnO nanocomposite under different annealing environments and photoswitchability. Journal of Applied Physics 112(6): 064308.
12. Seema S, Hari M, Pramod KS (2013) Polymer-supported titanium dioxide photocatalysts for environmental remediation: A review. Applied Catalysis A: General 462– 463: 178–195.
13. Park H, Park Y, Kim W, Choi W (2013) Surface modification of TiO_2 photocatalyst for environmental applications. Journal of Photochemistry and Photobiology C: Photochemistry Reviews 15: 1–20.
14. Zhang R, Zhong Q, Zhao W, Yu L, Qu H (2014) Promotional effect of fluorine on the selective catalytic reduction of NO with NH_3 over CeO_2-TiO_2 catalyst at low temperature. Applied Surface Science 289: 237–244.
15. Zhang H, Zong RL, Zhao J C, Zhu YF (2008) Dramatic Visible Photocatalytic Degradation Performances Due to Synergetic Effect of TiO_2 with PANI. Environmental Science & Technology 42: 3803–3807.
16. Lin YM, Li DZ, Hu JH, Xiao GC, Wang JX, Li WJ, et al. (2012) Highly Efficient Photocatalytic Degradation of Organic Pollutants by PANI-Modified TiO_2 Composite. The Journal of Physical Chemistry C 116: 5764–5772.
17. Li XY, Wang DS, Cheng GX, Luo QZ, An J, Wang Y. (2008) Preparation of polyaniline-modified TiO_2 nanoparticles and their photocatalytic activity under visible light illumination. Applied Catalysis B: Environmental 81: 267–273.
18. Wang DS, Wang YH, Li XY, Luo QZ, An J, Yue J (2008) Sunlight photocatalytic activity of polypyrrole-TiO_2 nanocomposites prepared by 'in situ' method. Catalysis Communications 9: 1162–1166.
19. Li XC, Jiang GL, He GH, Zheng W, Tan Y. Xiao W (2014) Preparation of porous PPy-TiO_2 composites: Improved visible light photoactivity and the mechanism. Chemical Engineering Journal 236: 480–489.
20. Wan-Kuen J, Hyun-Jung K (2013) (Ratios: 5, 10, 50, 100, and 200) Polyaniline-TiO_2 composites under visible- or UV-light irradiation for decomposition of organic vapors. Materials Chemistry and Physics 143: 247–255.

21. Ameen S, Akhtar MS, Kim GS, Kim YS, Yang OB, Shin HS (2009) Plasma-enhanced polymerized aniline/TiO_2 dye-sensitized solar cells. Journal of Alloys and Compounds 487: 382–386.
22. Seoudi R, Kamal M, Shabaka AA, Abdelrazek EM, Eisa W (2010) Synthesis, characterization and spectroscopic studies of CdS/polyaniline core/shell nanocomposite. Synthetic Metals 160: 479–484.
23. Mohamed A, Ahmed F, Ahmed B (2009) Photocatalytic degradation of Allura red and Quinoline yellow with Polyaniline/TiO_2 nanocomposite. Applied Catalysis B: Environmental 91: 59–66.
24. Rufford TE, Hulicova-Jurcakova D, Zhu ZH, Lu GQ (2008) Nanoporous carbon electrode from waste coffee beans for high performance supercapacitors. Electrochemistry Communications 10: 1594–1597.
25. Wang HL, Zhao DY, Jiang WF (2013) VIS-light-induced photocatalytic degradation of methylene blue (MB) dye using PoPD/TiO_2 composite photocatalysts. Desalination and Water Treatment 51(13–15): 2826–2835.
26. Shadpour M, Fariba D (2015) Functionalization of TiO_2 nanoparticles with bio-safe poly(vinyl alcohol) to obtain new poly(amide-imide) nanocomposites containing N,N'-(pyromellitoyl)-bis-L-leucine linkages. High Performance Polymers 27: 458–468.
27. Liao GZ, Chen S, Quan X, Zhang YB, Zhao HM (2011) Remarkable improvement of visible light photocatalysis with PANI modified core-shell mesoporous TiO_2 microspheres. Applied Catalysis B: Environmental 102: 126–131.
28. Liao GZ, Chen S, Quan X, Chen H, Zhang YB (2010) Photonic Crystal Coupled TiO_2/Polymer Hybrid for Efficient Photocatalysis under Visible Light Irradiation. Environmental Science & Technology 44: 3481–3485.
29. Li J, Peng T (2003) Response to high acidity and basicity at a platinum electrode in chronopotentiometry. Analytica Chimica Acta 478: 337–344.
30. Malitesta C, Palmisano F, Torsi L, Zambonin PG (1990) Glucose fast-response amperometric sensor based on glucose oxidase immobilized in an electropolymerized poly(o-phenylenediamine) film. Analytical Chemistry 62: 2735–2740. PMID: 2096737
31. Won-Hui J, Touseef A, Yu-Mi H, Hassan MS, Kim HC, Khil MS (2014) Novel PANI nanotube@TiO_2 composite as efficient chemical and biological disinfectant. Chemical Engineering Journal 246: 204–210.
32. Liang HC, Li XZ (2009) Visible-induced photocatalytic reactivity of polymer-sensitized titania nanotube films. Applied Catalysis B: Environmental 86: 8–17.
33. Csaba J, Wilaiwan C, Krishnan R (2014) Mechanistic Aspects of Photoelectrochemical Polymerization of Polypyrrole on a TiO_2 Nanotube Array. Electrochimica Acta 122: 303–309.
34. Yang JH, Wang DE, Han HX, Li C (2013) Roles of Cocatalysts in Photocatalysis and Photoelectrocatalysis. Accounts of Chemical Research 46: 1900–1909. https://doi.org/10.1021/ar300227e PMID: 23530781
35. Wang HL, Zhao DY, Jiang WF (2012) Synthesis and photocatalytic activity of poly-o-phenylenediamine (PoPD)/TiO_2 composite under VIS-light irradiation. Synthetic Metals 162: 296–302.
36. Wang YJ, Xu J, Zong WZ, Zhu Y (2011) Enhancement of photoelectric catalytic activity of TiO_2 film via polyaniline hybridization. Journal of Solid State Chemistry 184: 1433–1438.